

Probing the QCD phase transition with chiral mixing in dilepton production

Azumi Sakai,^{1,*} Masayasu Harada,^{2,3,4,†} Chiho Nonaka,^{1,2,3,5,‡}
Chihiro Sasaki,^{6,5,§} Kenta Shigaki,^{1,5,¶} and Satoshi Yano^{5,**}

¹*Physics Program, Hiroshima University, Higashi-Hiroshima, Hiroshima 739-8526, Japan*

²*Department of Physics, Nagoya University, Nagoya, Aichi 464-8602, Japan*

³*Kobayashi-Maskawa Institute for the Origin of Particles and the Universe,
Nagoya University, Nagoya, Aichi 464-8602, Japan*

⁴*Advanced Science Research Center, Japan Atomic Energy Agency, Tokai, Ibaraki 319-1195, Japan*

⁵*International Institute for Sustainability with Knotted Chiral Meta Matter (WPI-SKCM²),
Hiroshima University, Higashi-Hiroshima, Hiroshima 739-8526, Japan*

⁶*Institute of Theoretical Physics, University of Wrocław,
plac Maksa Borna 9, PL-50204 Wrocław, Poland*

(Dated: August 8, 2023)

We perform a systematic study of dilepton emission in a hot QCD medium based on three different scenarios of chiral mixing, each of which yields a characteristic structure in the vector spectral function. The in-medium spectral functions are accommodated into the state-of-the-art hydrodynamic simulations for a relativistic viscous fluid to calculate the dilepton production rate, fully accounting for the space-time evolution of a created fireball in relativistic heavy-ion collisions. We demonstrate that the low-temperature theorem of chiral mixing extrapolated toward a chiral crossover, often used in the literature, leads to critical shortcomings: the inadequacy of width broadening, and a substantial overestimate of the dilepton yield maximized around the invariant mass of $M = 1.2$ GeV. The proper prescription offers a milder yet sizable increase in the window of $1.1 < M < 1.4$ GeV as the direct signature of chiral symmetry restoration.

Introduction – Spontaneous breaking of chiral symmetry in Quantum Chromodynamics (QCD) is centered on dynamical mass generation of hadrons composed of light valence quarks. QCD matter created in relativistic heavy-ion collisions is a promising testing ground for exploring every change of hadron properties due to foreseen restoration of chiral symmetry driven by the QCD phase transition at high temperature and/or net-baryon density [1–4].

Short-lived vector mesons are of particular importance as they are anticipated to carry imprints of chiral symmetry restoration (CSR) which would emerge in dilepton production rates. In-medium modifications of the vector mesons are encoded in the spectral function, and the dilepton measurements in relativistic heavy-ion experiments indeed verified the existence of strong medium effects [5–8], although it remains inconclusive that the observed modifications could be quantified as the straightforward signature of CSR.

The ideal signature is the mass degeneracy of chiral partners carrying opposite parities. Especially favored is parity doubling of the ρ meson and its counterpart, a_1 meson, because of their short lifetimes compared to the fireball. However, the a_1 meson does not directly decay into a dilepton, so that its spectrum as a function of invariant mass is no longer possible to be reconstructed due to final state interactions.

A phenomenon called chiral mixing between vector and axial-vector states has hence attracted attention to overcome this experimental difficulty. The chiral mixing effect is induced via a soft pion interacting with ρ and a_1 states in a medium, and can be quantified in a model-

independent way at low temperature and/or density [9–11]. Consequently, the in-medium a_1 can be indirectly accessed in the ρ spectral function via the reactions of $a_1 + \pi \rightarrow \rho$ and $a_1 \rightarrow \rho + \pi$. Dilepton spectra are thus supposed to carry the mixing effect and its thermal evolution toward CSR at which the a_1 meson is expected to be equally massive to the ρ meson.

In the upcoming experiments at the CERN SPS [12] and the LHC [13], the measurement of CSR via chiral mixing is set with a high priority. In this letter, we shall address how different scenarios of CSR would possibly yield distinguishable results in the dilepton emission under the LHC condition.

There exist so far two major approaches to embed the chiral mixing into the in-medium spectral function. One is to go beyond the low-temperature theorem toward a critical temperature of CSR [14], leading to the chiral mixing *resolved* at CSR based on model-independent aspects of chiral dynamics. This is totally different from the naive expectation by extrapolating the mixing theorem to higher temperature, leading to a *maximal* mixing [15, 16]. The other is to build up the axial-vector spectrum from the Weinberg sum rules with a reliable vector spectrum, e.g. the one compatible with the experiments [17]. This approach requires some phenomenological assumptions, e.g. the energy dependence of the a_1 width as well as explicit inclusion of several low-lying states of vector mesons to saturate the sum rules. It is notable that the two approaches arrive at a more or less the same conclusion - a single distinct maximum in the vector spectrum indicating strongly the chiral mixing resolved at CSR, in the striking contrast to the result based

on the mixing theorem causing inevitably two maxima.

Another element to accurately assess the degree of the phenomenon is a reliable description of the space-time evolution of the medium created in relativistic heavy-ion collisions. Bulk properties of the medium described by hydrodynamic models, especially temperature, volume and lifetime, change dynamically in a short time scale, ~ 10 fm, and affect the dilepton yield. Since the expected difference of invariant mass spectra is rather subtle with and without the meson mass modifications in any of the scenarios, quantitative calculations anchored to firm field-theoretic bases are vital both in the QCD effective theories and hydrodynamic models. Given the fact that the contemporary modeling of hydrodynamic evolution of a hot medium with temperature dependent transport coefficients is at hand [18, 19], we shall combine it with the hadronic spectral functions with chiral mixing that develops as a function of temperature, to quantify the signatures of CSR relevant to the upcoming relativistic heavy-ion experiments.

Model – The differential rate of dilepton emission at finite temperature T from hadronic matter is related to the imaginary part of the vector-current correlation function G_V via

$$\frac{dR_{\text{had}}}{d^4q}(q;T) = \frac{\alpha_{\text{EM}}^2}{\pi^3 M^2} \frac{\text{Im}G_V(q;T)}{e^{q_0/T} - 1}, \quad (1)$$

where $\alpha_{\text{EM}} = e^2/4\pi$ represents the electromagnetic coupling constant and $M = \sqrt{q_0^2 - |\mathbf{q}|^2}$ the invariant mass with energy q_0 and three-momentum \mathbf{q} of a virtual photon. We shall construct the main input, the spectral function $\text{Im}G_V$, based on a prescription guiding the chiral mixing to the proper destination from low T towards the chiral crossover T_χ [14]. The interaction vertex of the ρ , a_1 and π mesons, responsible for the chiral mixing in a medium, is uniquely represented in terms of the mass difference, $\delta m = m_{a_1} - m_\rho$, or equivalently the pion decay constant f_π that is the order parameter of chiral symmetry breaking and its restoration. One readily finds that the chiral mixing vanishes at T_χ because of the degenerate ρ and a_1 states. In the following calculations, we will utilize a T -dependent δm which is vanishing toward T_χ with the mean-field critical exponent, as proposed in Ref. [14], whereas the ρ meson mass is kept constant throughout this paper. We note that the explicit breaking does not lead to a particular significance. Finite pion mass m_π results in a slight mass difference of $\delta m = 3$ MeV at T_χ , and the residual chiral mixing is negligible [14].

To differentiate the signature of CSR from the bulk, we consider three scenarios: (1) The case without CSR: Thermal corrections to the spectral function are encoded via meson loops, while δm is kept constant at any T . (2) The case with CSR: The in-medium spectral function is calculated with the thermal δm , leading to a gradual disappearance of the chiral mixing at higher T . (3)

The case with non-degenerate ρ and a_1 (hereafter “false CSR”): This relies crucially on the validity of the low-temperature theorem near T_χ . The model-independent formulae for G_V and its parity counterpart G_A are given at low $T \ll m_\pi$ by

$$\begin{aligned} G_V(q;T) &= (1 - \epsilon) G_V(q;0) + \epsilon G_A(q;0), \\ G_A(q;T) &= \epsilon G_V(q;0) + (1 - \epsilon) G_A(q;0), \end{aligned} \quad (2)$$

with $\epsilon = T^2/(6f_\pi^2)$ being the mixing parameter. When the ϵ could reach the maximal value of 1/2, $G_V = G_A$ would be realized at $T = \sqrt{3} f_\pi = 160$ MeV. The corresponding spectral functions would become identical as well, but this is a *fake* restoration. The reason is rather obvious: The restored symmetry requires the vanishing chiral mixing as explained above, and this ensures simultaneously the degenerate ρ and a_1 , the decay channel of $a_1 \rightarrow \rho\pi$ closed and the degenerate spectral functions in the vector and axial-vector sectors. The maximal mixing is clearly incompatible with the degenerate ρ and a_1 driven by a drastic change of QCD ground state emerging at the chiral phase transition. Thus, it fails to capture the non-trivial physics via a naive extrapolation of the low-temperature theorem. It is odd to occur, but based on the scenario with false CSR it is often argued that the chiral mixing generates an increase of the dilepton yield by 20–30% in the invariant mass between 1 and 1.4 GeV as a signature of CSR [15, 16].

Here we shall demonstrate how modifications due to the CSR emerge in the spectral function near T_χ , and quantify a relative difference among the three scenarios. Figure 1 shows the vector spectral function at various

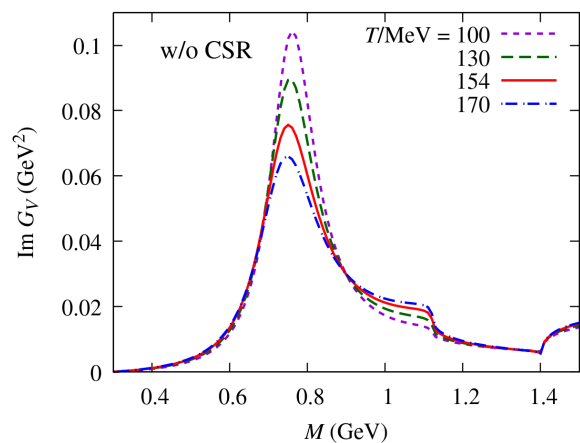


FIG. 1. (Color online). The temperature dependence of vector spectral function without chiral symmetry restoration. We improved the calculations done in Ref. [14] taking the updated value of $T_\chi = 154$ MeV determined in lattice QCD [20, 21].

temperatures without CSR but the chiral mixing fully implemented. The position of the ρ meson peak receives a slight shift due to the thermal effect produced mainly

via pion loops, whereas its strength is more reduced at higher T . The chiral mixing enters the vector spectrum via the a_1 - π loop diagrams, which results in the threshold effects above $M \simeq 1$ GeV: A shoulder at $M = m_{a_1} - m_\pi = 1.1$ GeV and a bump developing above $M = m_{a_1} + m_\pi = 1.4$ GeV arise due to two kinematically allowed processes, $\rho + \pi \rightarrow a_1$ and $\rho \rightarrow a_1 + \pi$, respectively [14]. Although the shape of the spectral function is somewhat modified, the locations of the ρ peak and the onset of threshold effects are unmodified. This is because the bare masses of ρ and a_1 states are set to be constant at any T , comprising the scenario without CSR as our baseline.

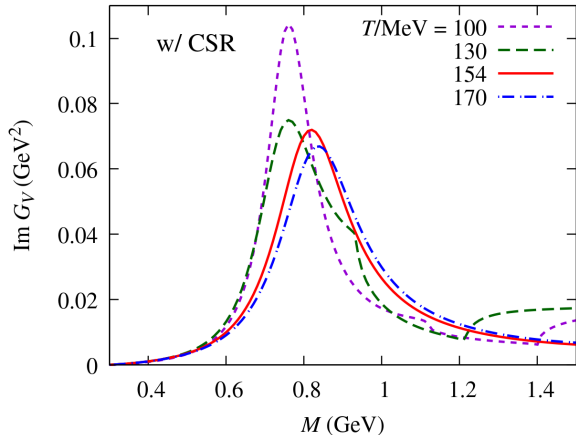


FIG. 2. (Color online). The same as in Fig. 1, but with chiral symmetry restoration.

The proper implementation of CSR modifies the vector spectrum substantially. One finds in Fig. 2 that the ρ peak is shifted upward and the onset of threshold effects downward at higher T . The former is induced by the pion-loop diagram carrying the coefficient of $(1 + m_\rho^2/m_{a_1}^2)$ which changes its strength as m_{a_1} approaches m_ρ . The latter appears also via the same physics, i.e. the a_1 meson becomes lighter. Those effects are eventually merged at T_χ to form a single maximum in the spectrum, clearly indicating the degenerate ρ and a_1 states.

Finally, the spectral function with the false CSR calculated from Eq. (2) is presented in Fig. 3. Since the entire thermal effects enter the current correlator only via the mixing parameter ϵ , a peak on the left for the ρ and a bump on the right for the a_1 do not change their pole positions, but do their strengths according to the mixing parameter ϵ at a given T . The spectral function in this scenario exhibits a striking contrast to the case with CSR shown in Fig. 2. There exists a clear overestimate at around $M = 1.2$ GeV, lying in the primary window of $1 < M < 1.4$ GeV where the totally distinct structure is found in Fig. 2.

The dilepton production rate is integrated over the whole space-time evolution of the medium created after

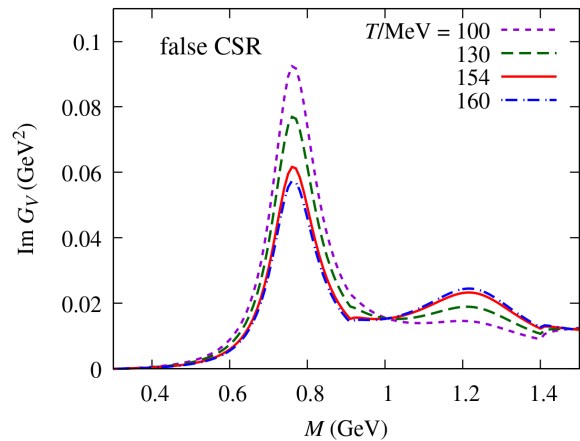


FIG. 3. (Color online). The same as in Fig. 1, but with false chiral symmetry restoration. The mixing parameter ϵ reaches $1/2$ at $T = 160$ MeV.

the collision. To describe a smooth crossover between the quark-gluon plasma (QGP) and hadronic phases at vanishing net-baryon density, we utilize a combined production rate proposed in Ref. [22]:

$$\frac{dR}{d^4q} = \frac{1}{2} \left(1 - \tanh \frac{T - T_\chi}{\Delta T} \right) \frac{dR_{\text{had}}}{d^4q} + \frac{1}{2} \left(1 + \tanh \frac{T - T_\chi}{\Delta T} \right) \frac{dR_{\text{QGP}}}{d^4q}, \quad (3)$$

with $\Delta T = 0.1T_\chi$. The dilepton emission rate from the QGP medium due to $\bar{q}q$ annihilation is given in the Born approximation by

$$\frac{d^4R_{\text{QGP}}}{d^4q}(q; T) = \frac{\alpha_{\text{EM}}^2}{6\pi^4} \frac{1}{e^{q^0/T} - 1} \left\{ 1 - \frac{2T}{|q|} \ln \left[\frac{n_-}{n_+} \right] \right\}, \quad (4)$$

$$n_\pm = 1 + \exp \left[-\frac{q^0 \pm |q|}{2T} \right]. \quad (5)$$

Results – We use the state-of-the-art model of relativistic viscous hydrodynamics to deal with a dynamic evolution of QCD matter [18] in which the bulk and shear viscosities depending on temperature are taken into account. A parametric initial condition model, TRENTo, is employed to obtain the profiles of initial entropy density [23, 24] with regulating the normalization parameter N and the interpolating parameter p between different initial conditions to reproduce the LHC data [19]. Equations of state in lattice QCD simulations, parameterized in the hadronic and QGP phases [25], are utilized. The hydrodynamic expansion starts at an initial time of $\tau_0 = 0.6$ fm under the assumption that thermal equilibrium is achieved by then. Our hydrodynamic calculations are carried out by generating 20 events for Pb+Pb collisions with the collision energy $\sqrt{s_{\text{NN}}} = 2.76$ TeV in the centrality window of 0–5%.

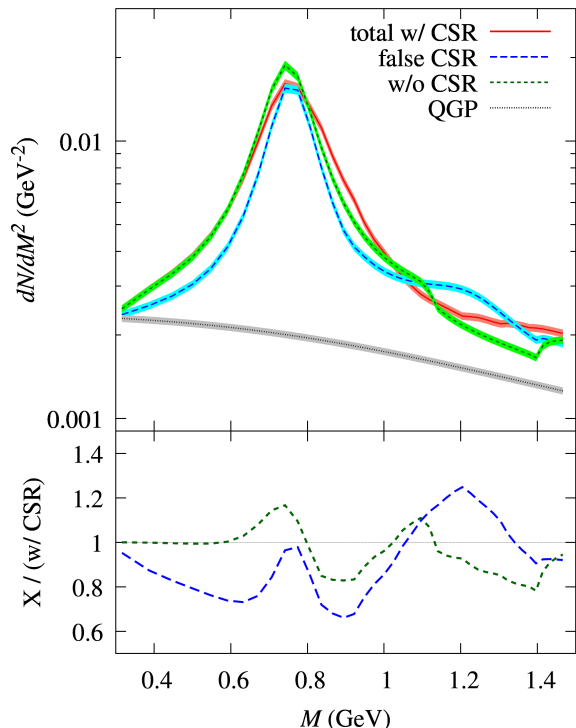


FIG. 4. (Color online). Upper panel: The total dilepton yields with the three hadronic spectral functions for Pb+Pb collisions with collision energy $\sqrt{s_{NN}} = 2.76$ TeV in the centrality 0–5%. The width of each line represents statistical errors. The dotted line is the rate from $\bar{q}q$ annihilation in the QGP medium. Lower panel: The production rates of the two scenarios, without CSR and false CSR, relative to the one with CSR.

Figure 4 shows the total dilepton yield calculated with the three hadronic spectra via Eq. (3), integrated over the rapidity η and transverse momenta p_T in the ranges of $|\eta| < 0.8$ and $0.2 < p_T < 5.0$ GeV. With the profile function [26] evaluated under the current assumption (3), the thermal dileptons produced in the hadronic phase amount to 70%. The structures seen in Figs. 1-3 persist in the overall yields for all the three cases. The consequences of CSR are observed above the ρ peak: an increase appears compared with the case without CSR in $0.8 < M < 1$ GeV, a window of the $a_1\rho\pi$ threshold effect operative, $1.1 < M < 1.4$ GeV, is filled in because of lighter a_1 , and those enhancements compensate a decrease at the ρ peak.

The production rate in the false CSR scenario exhibits a striking contrast to the proper CSR. The broadening effect is not captured at all. A substantial overestimate is found in $1.1 < M < 1.3$ GeV and becomes maximal at $M = 1.2$ GeV, amounting to a 25%-more contribution. Clearly, the enhancement is a fake signature of CSR emerging at the wrong place in M . This is traced back to the spectral function based on a naive superposition of the current correlators in matter-free-space, and

with which the mass difference between ρ and a_1 states, 0.47 GeV, is never resolved.

Confronted with the high-precision dimuon data by NA60 in Ref. [27], it was demonstrated that baryon effects via hadronic rescattering in a hot medium are vital to reproduce the data from the low to intermediate M region, whereas in $M > 0.8$ GeV there exists no such sensitivity. Therefore, our observation based on the spectral functions that do not include apparent effects from baryons, is anticipated to stay unchanged in a more realistic situation relevant to the ALICE experiments.

Summary – We studied the dilepton production in hot QCD based on two distinct scenarios of chiral symmetry restoration (CSR), fully taking account of space-time evolution of a created fireball in relativistic heavy-ion collisions under the LHC conditions. The scenario with CSR at which the degenerate ρ and a_1 is realized, leading to *vanishing* chiral mixing, was compared with the one in the false CSR scenario. This has been often referred in the literature based on the low-temperature theorem, leading to a *maximal* chiral mixing. We demonstrated that the two scenarios lead to distinct results as the signatures of CSR in dilepton production, especially in the most optimal window of invariant mass, $1 < M < 1.4$ GeV.

The false CSR model causes a fake contribution being maximal, 25% more than in the proper CSR scenario, and this becomes evident at $M = 1.24$ GeV, i.e. the vacuum a_1 mass. The correct model describes an enhancement of the rate in the window of $1.1 < M < 1.4$ GeV, such that the in-medium a_1 fills in this region separated by the onset of the $a_1\rho\pi$ threshold effect. The false CSR scenario also results in a sizable underestimate below and above the ρ peak due to the lack of broadening via meson loops.

Our result illustrates that the widely-accepted conjecture, based on a naive application of low-temperature theorem toward T_χ , should be interpreted with caution. The appropriate description of chiral mixing produces a somewhat moderate but yet sizable contribution directly related with the in-medium a_1 , and the signal is supposed to survive in a more realistic situation at small net-baryon density in view of the detailed study in a hadronic many-body approach [27].

In general, there exists a complicated admixture of two classes of chiral mixing in a hot and dense medium: One is the mixing effect considered in this study, and another is induced solely by baryon density [28, 29]. The latter never vanishes in striking contrast to the former, and results in a non-Breit-Wigner form of the vector spectral function emerging near the CSR, thus serving as the measurable signature in dilepton production in cold and dense matter [30, 31]. When a medium at moderate temperature and density is considered, it would be challenging to identify the effective chiral mixing implementing the both classes. The systematic study as performed in this letter is restricted in a hot and dilute medium, rele-

vant to the LHC physics, and the two mixing effects can be separated from one another only at such a limiting situation.

Acknowledgments – The work was supported in part by the World Premier International Research Center Initiative (WPI) under MEXT, Japan (CN, CS, KS, SY) and by Japan Society for the Promotion of Science (JSPS) KAKENHI Grant Nos. JP20K03927, JP23H05439 (MH), JP17K05438, JP20H00156, JP20H11581 (CN), JP18H05401 and JP20H00163 (KS). CS acknowledges the support by the Polish National Science Centre (NCN) under OPUS Grant Nos. 2018/31/B/ST2/01663 and 2022/45/B/ST2/01527. The numerical calculations were carried out on Yukawa-21 at YITP in Kyoto University, Japan.

* azumi-sakai@hiroshima-u.ac.jp

† harada@hken.phys.nagoya-u.ac.jp

‡ nchiho@hiroshima-u.ac.jp

§ chihiro.sasaki@uwr.edu.pl

¶ shigaki@hiroshima-u.ac.jp

** syano@hiroshima-u.ac.jp

- [1] R. S. Hayano and T. Hatsuda, Hadron properties in the nuclear medium, *Rev. Mod. Phys.* **82**, 2949 (2010), [arXiv:0812.1702 \[nucl-ex\]](#).
- [2] R. Rapp, J. Wambach, and H. van Hees, The Chiral Restoration Transition of QCD and Low Mass Dileptons, *Landolt-Bornstein* **23**, 134 (2010), [arXiv:0901.3289 \[hep-ph\]](#).
- [3] K. Fukushima and C. Sasaki, The phase diagram of nuclear and quark matter at high baryon density, *Prog. Part. Nucl. Phys.* **72**, 99 (2013), [arXiv:1301.6377 \[hep-ph\]](#).
- [4] A. Andronic, P. Braun-Munzinger, K. Redlich, and J. Stachel, Decoding the phase structure of QCD via particle production at high energy, *Nature* **561**, 321 (2018), [arXiv:1710.09425 \[nucl-th\]](#).
- [5] CERES Collaboration, e^+e^- pair production in Pb–Au collisions at 158-GeV per nucleon, *Eur. Phys. J. C* **41**, 475 (2005), [arXiv:0506002 \[nucl-ex\]](#).
- [6] NA60 Collaboration, First measurement of the ρ spectral function in high-energy nuclear collisions, *Phys. Rev. Lett.* **96**, 162302 (2006), [arXiv:0605007 \[nucl-ex\]](#).
- [7] STAR Collaboration, Dielectron mass spectra from au+au collisions at $\sqrt{s_{NN}}=200$ gev, *Phys. Rev. Lett.* **113**, 022301 (2014), [arXiv:0605007 \[nucl-ex\]](#).
- [8] PHENIX Collaboration, Dielectron production in au+au collisions at $\sqrt{s_{NN}}=200$ gev, *Phys. Rev. C* **93**, 014904 (2016), [arXiv:1509.04667 \[nucl-ex\]](#).
- [9] M. Dey, V. L. Eletsky, and B. L. Ioffe, Mixing of vector and axial mesons at finite temperature: an Indication towards chiral symmetry restoration, *Phys. Lett. B* **252**, 620 (1990).
- [10] G. Chanfray, J. Delorme, and M. Ericson, Chiral symmetry restoration and parity mixing, *Nucl. Phys. A* **637**, 421 (1998), [arXiv:nucl-th/9801020](#).
- [11] J. I. Kapusta and E. V. Shuryak, Weinberg type sum rules at zero and finite temperature, *Phys. Rev. D* **49**, 4694 (1994), [arXiv:hep-ph/9312245](#).
- [12] C. Ahdida et al. (NA60+), Letter of Intent: the NA60+ experiment, (2022), [arXiv:2212.14452 \[nucl-ex\]](#).
- [13] Letter of intent for ALICE 3: A next-generation heavy-ion experiment at the LHC, (2022), [arXiv:2211.02491 \[physics.ins-det\]](#).
- [14] M. Harada, C. Sasaki, and W. Weise, Vector-axialvector mixing from a chiral effective field theory at finite temperature, *Phys. Rev. D* **78**, 114003 (2008), [arXiv:0807.1417 \[hep-ph\]](#).
- [15] G. Usai et al. (NA60+), Study of hard and electromagnetic processes at CERN-SPS energies: an investigation of the high- μ_B region of the QCD phase diagram with NA60+, *JPS Conf. Proc.* **33**, 011113 (2021), [arXiv:1812.07948 \[nucl-ex\]](#).
- [16] F. Geurts and R.-A. Tripolt, Electromagnetic probes: Theory and experiment, *Prog. Part. Nucl. Phys.* **128**, 104004 (2023), [arXiv:2210.01622 \[hep-ph\]](#).
- [17] P. M. Hohler and R. Rapp, Is ρ -Meson Melting Compatible with Chiral Restoration?, *Phys. Lett. B* **731**, 103 (2014), [arXiv:1311.2921 \[hep-ph\]](#).
- [18] K. Okamoto and C. Nonaka, Temperature dependence of transport coefficients of QCD in high-energy heavy-ion collisions, *Phys. Rev. C* **98**, 054906 (2018), [arXiv:1712.00923 \[nucl-th\]](#).
- [19] H. Fujii, K. Itakura, K. Miyachi, and C. Nonaka, Radiative hadronization: Photon emission at hadronization from quark-gluon plasma, *Phys. Rev. C* **106**, 034906 (2022), [arXiv:2204.03116 \[nucl-th\]](#).
- [20] Y. Aoki, S. Borsanyi, S. Durr, Z. Fodor, S. D. Katz, S. Krieg, and K. K. Szabo, The QCD transition temperature: results with physical masses in the continuum limit II., *JHEP* **06**, 088, [arXiv:0903.4155 \[hep-lat\]](#).
- [21] A. Bazavov et al., The chiral and deconfinement aspects of the QCD transition, *Phys. Rev. D* **85**, 054503 (2012), [arXiv:1111.1710 \[hep-lat\]](#).
- [22] A. Monnai, Prompt, pre-equilibrium, and thermal photons in relativistic nuclear collisions, *J. Phys. G* **47**, 075105 (2020), [arXiv:1907.09266 \[nucl-th\]](#).
- [23] J. S. Moreland, J. E. Bernhard, and S. A. Bass, Alternative ansatz to wounded nucleon and binary collision scaling in high-energy nuclear collisions, *Phys. Rev. C* **92**, 011901 (2015), [arXiv:1412.4708 \[nucl-th\]](#).
- [24] W. Ke, J. S. Moreland, J. E. Bernhard, and S. A. Bass, Constraints on rapidity-dependent initial conditions from charged particle pseudorapidity densities and two-particle correlations, *Phys. Rev. C* **96**, 044912 (2017), [arXiv:1610.08490 \[nucl-th\]](#).
- [25] M. Bluhm, P. Alba, W. Alberico, A. Beraudo, and C. Ratti, Lattice QCD-based equations of state at vanishing net-baryon density, *Nucl. Phys. A* **929**, 157 (2014), [arXiv:1306.6188 \[hep-ph\]](#).
- [26] E. V. Shuryak, Quark-Gluon Plasma and Hadronic Production of Leptons, Photons and Psions, *Phys. Lett. B* **78**, 150 (1978).
- [27] H. van Hees and R. Rapp, Dilepton Radiation at the CERN Super Proton Synchrotron, *Nucl. Phys. A* **806**, 339 (2008), [arXiv:0711.3444 \[hep-ph\]](#).
- [28] S. K. Domokos and J. A. Harvey, Baryon number-induced Chern-Simons couplings of vector and axial-vector mesons in holographic QCD, *Phys. Rev. Lett.* **99**, 141602 (2007), [arXiv:0704.1604 \[hep-ph\]](#).
- [29] M. Harada and C. Sasaki, A Novel spectral broadening from vector-axial-vector mixing in dense matter, *Phys.*

- [Rev. C **80**, 054912 \(2009\)](#), [arXiv:0902.3608 \[hep-ph\]](#).
- [30] C. Sasaki, Signatures of chiral symmetry restoration in dilepton production, [Phys. Lett. B **801**, 135172 \(2020\)](#), [arXiv:1906.05077 \[hep-ph\]](#).
- [31] C. Sasaki, Anomaly-induced chiral mixing in cold and dense matter, [Phys. Rev. D **106**, 054034 \(2022\)](#), [arXiv:2207.00274 \[hep-ph\]](#).